NASA TN D-633

TECHNICAL NOTE

D-633

AN ANALYSIS OF THE FLAPWISE BENDING FREQUENCIES AND MODE SHAPES OF ROTOR BLADES HAVING TWO FLAPPING HINGES TO REDUCE VIBRATION LEVELS

By George W. Brooks and H. Wayne Leonard

Langley Research Center
Langley Field, Va.

NATIONAL AERONAUTICS AND SPACE ADMINISTRATION
WASHINGTON December 1960

NATIONAL AERONAUTICS AND SPACE ADMINISTRATION

TECHNICAL NOTE D-633

AN ANALYSIS OF THE FLAPWISE BENDING FREQUENCIES AND MODE SHAPES OF ROTOR BLADES HAVING TWO FLAPPING HINGES TO REDUCE VIBRATION LEVELS

By George W. Brooks and H. Wayne Leonard

SUMMARY

This paper presents the analysis of the flapwise natural bending frequencies and mode shapes of rotor blades with two flapping hinges located at arbitrary blade radii. The equations of motion are derived for a blade of variable mass and stiffness distribution. Solutions to the equations (natural frequencies and mode shapes) are presented for a typical blade of constant cross section having a wide range of hinge locations.

The results show that the natural frequencies of the blades can be changed appreciably by varying the locations of the blade hinges, and that with two properly located flapping hinges, blade designs are possible which eliminate or greatly reduce conditions of resonance between the blade natural frequencies and the frequencies of the harmonic air loads. The results also show that ratios of natural frequency to rotor speed below a value of 6.0 are essentially constant for variations in rotor speed consistent with helicopter and VTOL applications.

INTRODUCTION

Excessive vibrations in rotor craft have been cited as a major problem for many years. Currently, many operational helicopters have vibration levels which are too high for sustained fatigue-free operation, and others are penalized by having to carry the excess weight and mechanical complexity of tuned vibration dampers to hold the vibrations down to acceptable levels.

Although rotor craft are subject to several types of self-excited vibrations, the vibrations of primary concern are the forced vibrations which arise from the dynamic response of the structural components to the aerodynamic inputs. These inputs arise as a result of the movement

of the rotating rotor through the airstream and are transmitted to the structure proper through the blades. Thus, it seems expedient that further consideration be given to the nature and magnitude of the aerodynamic inputs and to the selection of blade designs having structural parameters which minimize adverse dynamic response. This paper deals with the latter problem, in that it presents a general method for the variation of the flapwise natural frequencies and mode shapes of the blades by the inclusion of multiple flapping hinges. An analysis is presented which treats both the rigid and elastic blade with two flapping hinges wherein the radial locations of the hinges and the spanwise distributions of mass and stiffness are completely general. The equations of motion are derived, and the natural frequencies and mode shapes are calculated for a blade of constant cross section for a wide range of flapping hinge locations and rotor speeds.

L
8
7
5

SYMBOLS

$a = \frac{a_2}{a_1}$

a_i ratio of spanwise location of ith flapping hinge to blade radius, measured along undeformed blade

b_i generalized coordinate for elastic bending of ith blade segment, in.

$(EI)_i$ blade flapwise bending stiffness distribution on ith blade segment, lb-in.^{2}

f_i first normal mode shape of ith blade segment when treated as a nonrotating beam with simply supported or hinged-hinged ends

$h_i = \frac{m_{i_0}}{m_{1_0}}$

i integer used to denote blade segment

j,p integer used as an index in summations

m_i mass per unit length of ith blade segment, lb-sec^2/in.^{2}

m_{i_0} value of m_i at inboard end of ith blade segment, lb-sec^2/in.^{2}

n	an integer used to denote mode number
N	number of blades
r	coordinate of blade element measured radially from center of rotor, in.
R	blade radius, in.
t	time, sec
T	total kinetic energy, lb-in.
T_i	contribution of ith blade segment to total kinetic energy, lb-in.
u_i	elastic deformation of ith blade segment in z-direction, in.
V	total potential energy, lb-in.
V_i	contribution of ith blade segment to total potential energy, lb-in.
x,y,z	Cartesian coordinates, in.
Z	total blade displacement in z-direction, normalized to maximum value
Δ	incremental change
η_i	coordinate of blade element in ith blade segment, measured from its inboard end, in.
μ_i	first natural frequency of nonrotating, hinged-hinged beam (corresponds to mode shape f_i), radians/sec
φ_i	generalized coordinate or flapping angle of ith blade segment with respect to (i - 1)th segment
ω	frequency of oscillation, radians/sec
ω_n	nth natural frequency of rotating blade, radians/sec
Ω	rotor angular velocity, radians/sec

Subscripts:

E elastic

R rigid

Dots over symbols denote differentiation with respect to time; primes denote differentiation with respect to r.

ANALYSIS

Derivation of the Equations of Motion

The coordinate system for the two-hinge elastic-segment blade is shown in figure 1. The x,y,z coordinate system is fixed in space and the position of a blade element of segment i (i = 0, 1, or 2) is given by

$$x_i = (r - \Delta r_i)\cos \Omega t \tag{1a}$$

$$y_i = (r - \Delta r_i)\sin \Omega t \tag{1b}$$

$$\left.\begin{aligned} z_0 &= 0 \\ z_i &= \sum_{j=1}^{i} (r - a_j R)\varphi_j + u_i(r,t) \qquad (i = 1,2) \end{aligned}\right\} \tag{1c}$$

where r is the radial location of a blade element measured along the undeformed blade, φ_i is the flapping angle between the ith blade segment and the nearest inboard segment, Δr_i is the distance the ith element moves toward the center of the rotor due to rotation and translation of the element as the blade deforms, and u_i is the elastic deformation of the ith blade segment in the z-direction. The inward movements of the elements of the respective blade segments are then given for small displacements by

$$\Delta r_0 = 0 \tag{2a}$$

$$\Delta r_1 = \frac{1}{2} \int_{a_1 R}^{r} \left(\varphi_1 + \frac{\partial u_1(r,t)}{\partial r}\right)^2 dr \tag{2b}$$

$$\Delta r_2 = \frac{1}{2}\int_{a_1R}^{a_2R}\left(\varphi_1 + \frac{\partial u_1(r,t)}{\partial r}\right)^2 dr + \frac{1}{2}\int_{a_2R}^{r}\left(\varphi_1 + \varphi_2 + \frac{\partial u_2(r,t)}{\partial r}\right)^2 dr \qquad (2c)$$

The deformation $u_i(r,t)$ can be represented by a summation of products of functions of time $b_{ij}(t)$ and deflection shapes $f_{ij}(r)$, that is, $u_i(r,t) = \sum_{j=1}^{p} b_{ij}(t)f_{ij}(r)$. For purposes of this investigation, only one term in the summation was used and upon dropping the second subscript, $f_i(r)$ was chosen as the first normal mode shape of a nonrotating beam identical to the ith blade segment simply supported at its ends (hereinafter referred to as hinged-hinged). The quantity $b_i(t)$ is then a generalized coordinate. Thus

$$u_i(r,t) \equiv b_i(t)f_i(r) \equiv b_i f_i \qquad (3)$$

and

$$\frac{\partial u_i(r,t)}{\partial r} = b_i(t)\frac{df_i(r)}{dr} \equiv b_i f_i' \qquad (4)$$

The positions of the elements of the respective blade segments in the coordinate system are given by substitution of the proper expressions for $\frac{\partial u_i(r,t)}{\partial r}$ into equations (2) and the resulting expressions for Δr_i into equations (1). For example,

$$x_2 = (r - \Delta r_2)\cos \Omega t = \left[r - \frac{1}{2}\int_{a_1R}^{a_2R}(\varphi_1 + b_1 f_1')^2 dr - \frac{1}{2}\int_{a_2R}^{r}(\varphi_1 + \varphi_2 + b_2 f_2')^2 dr\right]\cos \Omega t \qquad (a_2R \leq r \leq R)$$

The kinetic and potential energies of each blade segment may now be calculated and summed to obtain the total kinetic energy T, that is,

$$T = T_0 + T_1 + T_2 \qquad (5a)$$

$$T = \frac{1}{2} \int_0^R m\left(\dot{x}^2 + \dot{y}^2 + \dot{z}^2\right)dr \tag{5b}$$

$$T = \frac{1}{2}\left[\int_0^{a_1R} m_0\left(\dot{x}_0^2 + \dot{y}_0^2 + \dot{z}_0^2\right)dr + \int_{a_1R}^{a_2R} m_1\left(\dot{x}_1^2 + \dot{y}_1^2 + \dot{z}_1^2\right)dr + \int_{a_2R}^{R} m_2\left(\dot{x}_2^2 + \dot{y}_2^2 + \dot{z}_2^2\right)dr\right] \tag{5c}$$

and the total potential energy V

$$V = V_0 + V_1 + V_2 \tag{6a}$$

$$V = 0 + \frac{b_1^2}{2} \int_{a_1R}^{a_2R} (EI)_1\left(f_1''\right)^2 dr + \frac{b_2^2}{2} \int_{a_2R}^{R} (EI)_2\left(f_2''\right)^2 dr \tag{6b}$$

At this point, the straightforward approach would be to calculate the three components of deflection for each blade segment, differentiate and integrate as indicated in equations (5c) and (6b), and thus obtain the complete energy expressions. However, a better approach which will considerably simplify the problem is to apply Lagrange's equation at this stage, that is, to derive the equations of motion in symbolic form. Thus for each generalized coordinate represented by q_s the following equation is derived:

$$\frac{d}{dt}\left(\frac{\partial T}{\partial \dot{q}_s}\right) - \frac{\partial T}{\partial q_s} + \frac{\partial V}{\partial q_s} = 0 \tag{7}$$

where q_s denotes any one of the generalized coordinates φ_1, φ_2, b_1, or b_2. Then

$$\frac{d}{dt}\left(\frac{\partial T}{\partial \dot{q}_s}\right) = \int_0^{a_1R} m_0\left[\ddot{x}_0 \frac{\partial \dot{x}_0}{\partial \dot{q}_s} + \dot{x}_0 \frac{d}{dt}\left(\frac{\partial \dot{x}_0}{\partial \dot{q}_s}\right) + \ddot{y}_0 \frac{\partial \dot{y}_0}{\partial \dot{q}_s} + \dot{y}_0 \frac{d}{dt}\left(\frac{\partial \dot{y}_0}{\partial \dot{q}_s}\right) + \ddot{z}_0 \frac{\partial \dot{z}_0}{\partial \dot{q}_s} + \dot{z}_0 \frac{d}{dt}\left(\frac{\partial \dot{z}_0}{\partial \dot{q}_s}\right)\right] dr$$

$$+ \int_{a_1R}^{a_2R} m_1\left[\ddot{x}_1 \frac{\partial \dot{x}_1}{\partial \dot{q}_s} + \dot{x}_1 \frac{d}{dt}\left(\frac{\partial \dot{x}_1}{\partial \dot{q}_s}\right) + \ddot{y}_1 \frac{\partial \dot{y}_1}{\partial \dot{q}_s} + \dot{y}_1 \frac{d}{dt}\left(\frac{\partial \dot{y}_1}{\partial \dot{q}_s}\right) + \ddot{z}_1 \frac{\partial \dot{z}_1}{\partial \dot{q}_s} + \dot{z}_1 \frac{d}{dt}\left(\frac{\partial \dot{z}_1}{\partial \dot{q}_s}\right)\right] dr$$

$$+ \int_{a_2R}^{R} m_2\left[\ddot{x}_2 \frac{\partial \dot{x}_2}{\partial \dot{q}_s} + \dot{x}_2 \frac{d}{dt}\left(\frac{\partial \dot{x}_2}{\partial \dot{q}_s}\right) + \ddot{y}_2 \frac{\partial \dot{y}_2}{\partial \dot{q}_s} + \dot{y}_2 \frac{d}{dt}\left(\frac{\partial \dot{y}_2}{\partial \dot{q}_s}\right) + \ddot{z}_2 \frac{\partial \dot{z}_2}{\partial \dot{q}_s} + \dot{z}_2 \frac{d}{dt}\left(\frac{\partial \dot{z}_2}{\partial \dot{q}_s}\right)\right] dr \qquad (8a)$$

$$\frac{\partial T}{\partial q_s} = \int_0^{a_1R} m_0\left[\dot{x}_0 \frac{\partial \dot{x}_0}{\partial q_s} + \dot{y}_0 \frac{\partial \dot{y}_0}{\partial q_s} + \dot{z}_0 \frac{\partial \dot{z}_0}{\partial q_s}\right] dr$$

$$+ \int_{a_1R}^{a_2R} m_1\left[\dot{x}_1 \frac{\partial \dot{x}_1}{\partial q_s} + \dot{y}_1 \frac{\partial \dot{y}_1}{\partial q_s} + \dot{z}_1 \frac{\partial \dot{z}_1}{\partial q_s}\right] dr$$

$$+ \int_{a_2R}^{R} m_2\left[\dot{x}_2 \frac{\partial \dot{x}_2}{\partial q_s} + \dot{y}_2 \frac{\partial \dot{y}_2}{\partial q_s} + \dot{z}_2 \frac{\partial \dot{z}_2}{\partial q_s}\right] dr \qquad (8b)$$

and

$$\frac{\partial V}{\partial q_s} = \frac{\partial}{\partial q_s}\left[\frac{b_1^2}{2} \int_{a_1R}^{a_2R} (EI)_1 (f_1'')^2 dr + \frac{b_2^2}{2} \int_{a_2R}^{R} (EI)_2 (f_2'')^2 dr\right] \qquad (8c)$$

The integrals in equation (8c) are given in terms of the radial distribution of the blade flexural rigidity EI, and the second derivatives of the flexural deformation f. These integrals may also be written in terms of the natural frequencies of the nonrotating hinged-hinged segments having the mass distributions m and the modal deformations f, that is,

$$\int_{a_1R}^{a_2R} (EI)_1 (f_1'')^2 dr = \mu_1^2 \int_{a_1R}^{a_2R} m_1 f_1^2 dr$$

and

$$\int_{a_2R}^{R} (EI)_2 (f_2'')^2 dr = \mu_2^2 \int_{a_2R}^{R} m_2 f_2^2 \, dr$$

This form is useful in that the potential energy in equation (8c) can be written in terms of the more readily determined quantities μ_i, f_i, and m_i rather than $(EI)_i$ and f_i''. This substitution is used in the remainder of the report.

The equations of motion for the respective generalized coordinates, after appropriate differentiations and rearrangement, and with only linear terms retained are:

$$\ddot{\varphi}_1 \left[\int_{a_1R}^{a_2R} m_1 (r - a_1R)^2 dr + \int_{a_2R}^{R} m_2 (r - a_1R)^2 dr \right] + \Omega^2 \varphi_1 \left[\int_{a_1R}^{a_2R} \left(m_1 r \int_{a_1R}^{r} dr \right) dr + \int_{a_2R}^{R} \left(m_2 r \int_{a_1R}^{r} dr \right) dr \right]$$

$$+ \ddot{\varphi}_2 \left[\int_{a_2R}^{R} m_2 (r - a_1 r)(r - a_2R) dr \right] + \Omega^2 \varphi_2 \left[\int_{a_2R}^{R} \left(m_2 r \int_{a_2R}^{r} dr \right) dr \right] + \ddot{b}_1 \left[\int_{a_1R}^{a_2R} m_1 (r - a_1R) f_1 \, dr \right]$$

$$+ \Omega^2 b_1 \left[\int_{a_1R}^{a_2R} \left(m_1 r \int_{a_1R}^{r} f_1' \, dr \right) dr \right] + \ddot{b}_2 \left[\int_{a_2R}^{R} m_2 (r - a_1R) f_2 \, dr \right] + \Omega^2 b_2 \left[\int_{a_2R}^{R} \left(m_2 r \int_{a_2R}^{r} f_2' \, dr \right) dr \right] = 0 \qquad (9a)$$

$$\ddot{\varphi}_1 \left[\int_{a_2R}^{R} m_2 (r - a_1R)(r - a_2R) dr \right] + \Omega^2 \varphi_1 \left[\int_{a_2R}^{R} \left(m_2 r \int_{a_2R}^{r} dr \right) dr \right] + \ddot{\varphi}_2 \left[\int_{a_2R}^{R} m_2 (r - a_2R)^2 dr \right]$$

$$+ \Omega^2 \varphi_2 \left[\int_{a_2R}^{R} \left(m_2 r \int_{a_2R}^{r} dr \right) dr \right] + \ddot{b}_2 \left[\int_{a_2R}^{R} m_2 (r - a_2R) f_2 \, dr \right] + \Omega^2 b_2 \left[\int_{a_2R}^{R} \left(m_2 r \int_{a_2R}^{r} f_2' \, dr \right) dr \right] = 0 \qquad (9b)$$

$$\ddot{\varphi}_1 \left[\int_{a_1R}^{a_2R} m_1 f_1 (r - a_1R) dr \right] + \Omega^2 \varphi_1 \left[\int_{a_1R}^{a_2R} \left(m_1 r \int_{a_1R}^{r} f_1' \, dr \right) dr \right] + \ddot{b}_1 \left[\int_{a_1R}^{a_2R} m_1 f_1^2 \, dr \right]$$

$$+ \Omega^2 b_1 \left[\int_{a_1R}^{a_2R} \left(m_1 r \int_{a_1R}^{r} (f_1')^2 dr \right) dr + \int_{a_2R}^{R} \left(m_2 r \int_{a_1R}^{a_2R} (f_1')^2 dr \right) dr \right]$$

$$+ \mu_1^2 b_1 \left[\int_{a_1R}^{a_2R} m_1 f_1^2 \, dr \right] = 0 \qquad (9c)$$

$$\ddot{\varphi}_1\left[\int_{a_2R}^{R} m_2(r - a_1R)f_2\,dr\right] + \Omega^2\varphi_1\left[\int_{a_2R}^{R}\left(m_2r\int_{a_2R}^{r} f_2'\,dr\right)dr\right]$$

$$+ \ddot{\varphi}_2\left[\int_{a_2R}^{R} m_2(r - a_2R)f_2\,dr\right] + \Omega^2\varphi_2\left[\int_{a_2R}^{R}\left(m_2r\int_{a_2R}^{r} f_2'\,dr\right)dr\right]$$

$$+ \ddot{b}_2\left[\int_{a_2R}^{R} m_2 f_2^2\,dr\right] + \Omega^2 b_2\left[\int_{a_2R}^{R}\left(m_2r\int_{a_2R}^{r}(f_2')^2 dr\right)dr\right]$$

$$+ b_2\mu_2^2\left[\int_{a_2R}^{R} m_2 f_2^2\,dr\right] = 0 \qquad (9d)$$

Equations (9) are now written in matrix form. For convenience, the integrals contained in each square bracket of equations (9) have been nondimensionalized and expressed in terms of coefficients A_{11}, B_{11}, and so forth. In order to nondimensionalize the integrals, equations (9a) and (9b) were divided by $\Omega^2 m_{1_0} R^3$ and equations (9c) and (9d) were divided by $\Omega^2 m_{1_0} R^2$. It is also assumed that the blade motions are harmonic. The resulting equation is

$$
\begin{bmatrix}
-\left(\frac{\omega}{\Omega}\right)^2(A_{11}+B_{11}h_2)+E_{11}+F_{11}h_2 & -\left(\frac{\omega}{\Omega}\right)^2 B_{12}h_2+F_{12}h_2 & -\left(\frac{\omega}{\Omega}\right)^2 A_{13}+E_{13} & -\left(\frac{\omega}{\Omega}\right)^2 B_{14}h_2+F_{14}h_2 \\
-\left(\frac{\omega}{\Omega}\right)^2 B_{12}h_2+F_{12}h_2 & -\left(\frac{\omega}{\Omega}\right)^2 B_{22}h_2+F_{12}h_2 & 0 & -\left(\frac{\omega}{\Omega}\right)^2 B_{24}h_2+F_{14}h_2 \\
-\left(\frac{\omega}{\Omega}\right)^2 A_{13}+E_{13} & 0 & -\left(\frac{\omega}{\Omega}\right)^2 A_{33}+E_{33}+F_{33}h_2+\left(\frac{\mu_1}{\Omega}\right)^2 A_{33} & 0 \\
-\left(\frac{\omega}{\Omega}\right)^2 B_{14}h_2+F_{14}h_2 & -\left(\frac{\omega}{\Omega}\right)^2 B_{24}h_2+F_{14}h_2 & 0 & -\left(\frac{\omega}{\Omega}\right)^2 B_{44}h_2+F_{44}h_2+\left(\frac{\mu_2}{\Omega}\right)^2 B_{44}h_2
\end{bmatrix}
\begin{Bmatrix} \varphi_1 \\ \varphi_2 \\ b_{1/R} \\ b_{2/R} \end{Bmatrix}
=
\begin{Bmatrix} 0 \\ 0 \\ 0 \\ 0 \end{Bmatrix}
\qquad (10)
$$

Note that the coefficients A_{11}, B_{11}, and so forth of equation (10) are completely general with respect to the mass and stiffness distributions and the hinged-hinged mode shapes of the segments. For example, some expressions for the coefficients are:

$$A_{11} = \frac{1}{R^3}\int_{a_1R}^{a_2R} \frac{m_1}{m_{1_0}}(r - a_1R)^2 dr$$

$$B_{11} = \frac{1}{R^3}\int_{a_2R}^{R} \frac{m_2}{m_{2_0}}(r - a_1R)^2 dr$$

$$F_{14} = \frac{1}{R^2} \int_{a_2R}^{R} \left(\frac{m_2}{m_{2_0}} r \int_{a_2R}^{r} f_2' \, dr \right) dr$$

$$h_2 = \frac{m_{2_0}}{m_{1_0}}$$

Evaluation of Coefficients for Uniform Segments

If the mass and stiffness distributions of each segment are constant throughout its length, the first natural-mode shapes for elastic bending of the hinged-hinged segments are given by

$$f_1 \equiv f_1(r) = \sin \pi \frac{\eta_1}{R(a_2 - a_1)} \qquad \left(0 < \eta_1 < R(a_2 - a_1)\right) \qquad \text{(11a)}$$

$$f_2 \equiv f_2(r) = \sin \pi \frac{\eta_2}{R(1 - a_2)} \qquad \left(0 < \eta_2 < R(1 - a_2)\right) \qquad \text{(11b)}$$

Then, for example, the integral $\int_{a_1R}^{a_2R} f_1 r \, dr$ can be expressed as follows:

$$\int_{a_1R}^{a_2R} f_1 r \, dr = \int_{0}^{R(a_2-a_1)} f_1(a_1R + \eta_1)\,(a_1R + \eta_1) d\eta_1$$

$$= a_1R \int_{0}^{R(a_2-a_1)} \sin \frac{\eta_1 \pi}{R(a_2 - a_1)} \, d\eta_1$$

$$+ \int_{0}^{R(a_2-a_1)} \eta_1 \sin \frac{\eta_1 \pi}{R(a_2 - a_1)} \, d\eta_1$$

The coefficients of the matrix (eq. (10)) are given by the following expressions:

$$A_{11} = \frac{a_1^3}{3}(a - 1)^3$$

$$A_{13} = \frac{a_1^2}{\pi}(a - 1)^2$$

$$A_{33} = \frac{a_1}{2}(a - 1)$$

$$B_{11} = \frac{1}{3}(1 - aa_1)\left(1 + a^2a_1^2 + aa_1 - 3aa_1^2 + 3a_1^2\right)$$

$$B_{12} = \frac{1}{3}(1 - aa_1)\left(1 - \frac{1}{2}aa_1 - \frac{1}{2}a^2a_1^2 - \frac{3}{2}a_1 + \frac{3}{2}aa_1^2\right)$$

$$B_{14} = \frac{1}{\pi}(1 - aa_1)(1 + aa_1 - 2a_1)$$

$$B_{22} = \frac{1}{3}(1 - aa_1)^3$$

$$B_{24} = \frac{1}{\pi}(1 - aa_1)^2$$

$$B_{44} = \frac{1}{2}(1 - aa_1)$$

$$E_{11} = \frac{1}{3}a_1^3\left(a^3 - \frac{3}{2}a^2 + \frac{1}{2}\right)$$

$$E_{13} = \frac{a_1^2}{\pi}(a^2 - 1)$$

$$E_{33} = a_1\frac{\pi^2}{24}\left[a\left(4 - \frac{3}{\pi^2}\right) + \left(2 + \frac{3}{\pi^2}\right)\right]$$

$$F_{11} = \frac{1}{3}\left(1 - aa_1\right)\left(1 - \frac{3}{2}a_1 + aa_1 - \frac{3}{2}aa_1^2 + a^2a_1^2\right)$$

$$F_{12} = \frac{1}{3}\left(1 - aa_1\right)\left(1 - \frac{1}{2}aa_1 - \frac{1}{2}a^2a_1^2\right)$$

$$F_{13} = 0$$

$$F_{14} = \frac{1}{\pi}\left(1 - a^2a_1^2\right)$$

$$F_{33} = \frac{\pi^2}{4a_1}\left(\frac{1 - a^2a_1^2}{a - 1}\right)$$

$$F_{44} = \frac{\pi^2}{24}\left[aa_1\left(2 + \frac{3}{\pi^2}\right) + \left(4 - \frac{3}{\pi^2}\right)\right]$$

$$\mu_1^2 = \frac{\pi^4}{R^4\left(a_2 - a_1\right)^4}\frac{(EI)_1}{m_1}$$

$$\mu_2^2 = \frac{\pi^4}{R^4\left(1 - a_2\right)^4}\frac{(EI)_2}{m_2}$$

DISCUSSION OF RESULTS

This section of the report treats both the rigid-segment blade $\left(b_1 = b_2 = 0\right)$ and the flexible-segment blade to determine (a) the variation of natural frequencies with rotor speed, (b) the variation of the natural frequencies with hinge locations, (c) a comparison of the natural frequencies of the flexible-segment blade with those of the rigid-segment blade, and (d) the effect of rotor speed and hinge locations on the natural mode shapes.

For purposes of illustration, it was assumed in obtaining the calculated results subsequently presented that the mass and stiffness distributions are uniform throughout the length of the blade outboard of the inboard flapping hinge, and the values used $\left(m_1 = m_2 = 0.6 \times 10^{-3}\ \frac{\text{lb-sec}^2}{\text{in}^2};\ (EI)_1 = (EI)_2 = 3.15 \times 10^6\ \text{lb-in.}^2;\right.$ and $\left.R = 210\ \text{in.}\right)$ are typical of those of a medium-size helicopter.

Rigid-Segment Blade

The natural frequencies of the rigid-segment blade are obtained by the vanishing of the determinant of the submatrix formed by eliminating the third and fourth rows and third and fourth columns of equation (10). The natural frequencies of the resulting two-degree-of-freedom system for a blade of uniform cross section are given in table I. The frequency ratio, obtained by dividing by the rotor speed, is also plotted as a function of hinge locations in figure 2 where the abscissa is the radial location of the second hinge point. Calculations are presented for inboard hinge locations of 4 percent, 10 percent, and 30 percent of the radius.

One of the significant features of the multihinged rigid-segment blade is that the natural frequency of a given mode is always a constant multiple of the rotor speed and consequently blade designs are possible which will eliminate conditions of resonance between the blade natural frequencies and the frequencies of the harmonic aerodynamic loads as the rotor speed is varied.

The mode shapes for the rigid-segment blade are obtained by substitution of the natural frequencies or roots presented in table I back into either of the first two equations of the submatrix and solving for the ratio φ_1/φ_2. This ratio, which is independent of rotor speed, was calculated for several practical hinge configurations and the results are presented in the following table:

a_1	a_2	$\frac{\omega_n}{\Omega}$	n	$\frac{\varphi_1}{\varphi_2}$
0.04	0.40	1.031	1	50.442
.04	.40	3.018	2	-.464
.10	.50	1.080	1	20.389
.10	.50	3.050	2	-.378
.30	.60	1.279	1	7.067
.30	.60	3.615	2	-.400

The two mode shapes for the configuration where $a_1 = 0.04$ and $a_2 = 0.40$ are plotted in figure 3.

Figure 3 shows that the blade segments aline themselves during vibration in a manner which resembles the flapping and first elastic bending modes of a conventional rotor. However, the radial locations of the node and antinode for the second mode are directly dependent on the hinge locations and move toward the tip as a_2 approaches unity.

Elastic-Segment Blade

If the flexibilities of the various segments of a rotor blade with two flapping hinges are neglected, the system, as shown in the previous section, reduces to a two-degree-of-freedom system. Thus, two natural modes with their associated natural frequencies are obtained. If, however, the segments are considered to be flexible, two primary effects result. The first effect is that additional degrees of freedom are obtained, the number of which is equal to twice the number of elastic modes of deformation assumed for each segment. The coupling of these additional degrees of freedom with the flapping modes results in higher natural modes and frequencies of the blade.

A second result is that the natural frequencies of the lower two modes, which are constituted primarily of flapping of the blade segments about the hinges, are subject to change. The effect of flexibility of the segments on the lower frequencies can then be observed for any configuration of hinge locations by comparing the first two natural frequencies of the flexible-segment blade with the respective frequencies for the rigid-segment blade.

The study made in the present paper treats the case where each blade segment is permitted one degree of freedom in flexure defined by the first natural mode of the appropriate hinged-hinged segment. The four natural frequencies for the blade, as well as the frequency ratios obtained by dividing by the rotor speed, are presented in table II for various rotor speeds and hinge locations. The ratios of the natural frequencies to the rotor speed for the first three modes are plotted in figures 4. The natural frequencies for the fourth mode are generally above the values of practical interest in rotor design (see table II) and are therefore omitted from the figures.

A comparison of the frequency curves presented in figures 4 shows that the ratio of ω_1/Ω is independent of either rotor speed or the spanwise location of the outboard hinge but increases as the inboard hinge is moved outward. In the case of the second mode, a small dependence of ω_2/Ω on both rotor speed and hinge locations is shown. The frequency ratio is increased as the rotor speed is reduced and also as the second hinge location is moved in either direction from the point where the outer two segments of the blade are of approximately equal length. The frequencies of the second mode are also increased as the inboard hinge is moved toward the blade tip. Figure 4 also shows that the natural frequencies for the third mode are highly dependent on both the hinge locations and the rotor speed.

From flight-operations experience, aerodynamic excitations have been found to occur at integer multiples of the rotor speed, and the

excitations are more severe when the integer is a lower multiple of the number of blades. Thus, in order to minimize structural amplifications due to resonance, it is desirable to choose the hinge locations so that resonant frequencies are avoided. In consideration of the two-blade rotor, for example, one should select a value of a_1 as large as possible (consistent with rotor moment requirements for stability and control) to raise the natural frequency of the second mode so that $3 < \frac{\omega_2}{\Omega} < 4$ and to choose a value of a_2 such that ω_3/Ω is both as high and as far removed from integer values as possible.

For helicopter applications and for the blade parameters selected, $\Omega \approx 30$. Thus, it appears that desirable values for a_1 and a_2 for blades having the chosen values of EI and m would be 0.30 and 0.54, respectively. For VTOL applications, it may be desirable to vary the rotor speed substantially during the flight, and in this case it would be desirable to select hinge configurations which minimize resonance conditions at lower rotor harmonics throughout the range of rotor speeds. These conditions also suggest a large value of a_1, perhaps 0.25, and a value of a_2 of about 0.80. Although it may be impossible to avoid some resonances involving the third-mode natural frequencies during the variations of rotor speed, at least they occur at higher harmonics where the excitation forces are usually small.

For design purposes, primary concern is usually exercised over the natural frequencies in the neighborhood of the first two modes. The problem of calculating the natural frequencies for the rigid-segment blade is relatively simple, and the question of accounting for the effects of rotor speed and segment elasticity are then of interest. The effects of these variables on the natural frequencies of the first two modes are shown in figure 5 where the ratios of the natural frequencies for the elastic-segment blade to the frequencies for the rigid-segment blade $(\omega_n)_E/(\omega_n)_R$ where n = 1 and 2 are presented. The curves show that no perceptible differences exist for the first mode but that the second-mode frequencies of the elastic-segment blade may be substantially less than those for the rigid-segment blade, particularly for high rotor speeds and for outboard hinge locations for which the ratios of the lengths of the hinged segments are substantially different from unity. The effect of inboard hinge location is small. For helicopter applications and for hinged segments of approximately equal length, the second natural frequency for the elastic-segment blade is approximately 94 percent of the value predicted for the rigid-segment blade.

The modal coefficients for some typical cases for the elastic-segment blade are presented in table III, and the four modes are plotted

for a typical configuration in figure 6. The dashed lines indicate the deformations of the blade as a result of rotations of the blade segments about the hinges, and the vertical distances between the solid and dashed lines indicate the deformations due to elastic bending. If the inboard hinge is considered as a node, the curves show that the modal number is equal to the number of nodes. It may also be noted that the higher blade elastic deformations for the lower modes occur on the outboard segment.

CONCLUDING REMARKS

A method of analysis is presented and applied to the determination of the natural frequencies and mode shapes of rotor blades having two flapping hinges. The equations of motion are derived and put in matrix form for the general case of a rotor blade having any radial variation of mass, stiffness, and/or hinge locations.

The results of this study indicate that the ratios of the natural flapwise bending frequencies of the rotor blade to the rotor speed ω_n/Ω may be substantially controlled by proper choice of hinge locations. In fact one of the significant features of the rigid-segment blade is that the natural frequency of a given mode is always a constant multiple of the rotor speed and consequently blade designs are possible which will eliminate conditions of resonance between the blade natural frequencies and the frequencies of the harmonic loads as the rotor speed is varied. The results of the study also show that for the elastic-segment blade both ω_1/Ω and ω_2/Ω are essentially independent of rotor speed for realistic hinge configurations. When the outboard hinge was situated about half way between the inboard hinge and the blade tip, it was found for the example case treated that the natural frequency for the second mode of the elastic-segment blade was only about 3 to 6 percent lower than the value obtained when the blade segments were assumed to be rigid.

Langley Research Center,
National Aeronautics and Space Administration,
Langley Field, Va., September 16, 1960.

TABLE I

NATURAL FREQUENCIES FOR TWO-HINGE RIGID-SEGMENT BLADE

$$\left[m_1 = m_2 = 0.6 \times 10^{-3} \frac{\text{lb-sec}^2}{\text{in.}^2}\right]$$

Ω, radians/sec	a_1	a_2	ω_1, radians/sec	ω_2, radians/sec	$\frac{\omega_1}{\Omega}$	$\frac{\omega_2}{\Omega}$
8	0.04	0.20	8.246	31.699	1.031	3.962
16	.04	.20	16.492	63.399	1.031	3.962
24	.04	.20	24.738	95.098	1.031	3.962
32	.04	.20	32.984	126.797	1.031	3.962
8	.04	.40	8.246	24.147	1.031	3.018
16	.04	.40	16.492	48.294	1.031	3.018
24	.04	.40	24.738	72.440	1.031	3.018
32	.04	.40	32.983	96.587	1.031	3.018
8	.04	.60	8.246	23.052	1.031	2.881
16	.04	.60	16.492	46.104	1.031	2.881
24	.04	.60	24.738	69.156	1.031	2.881
32	.04	.60	32.984	92.208	1.031	2.881
8	.04	.80	8.246	26.630	1.031	3.329
16	.04	.80	16.492	53.261	1.031	3.329
24	.04	.80	24.738	79.891	1.031	3.329
32	.04	.80	32.985	106.522	1.031	3.329
8	.10	.30	8.639	29.871	1.080	3.734
16	.10	.30	17.278	59.743	1.080	3.734
24	.10	.30	25.917	89.614	1.080	3.734
32	.10	.30	34.556	119.486	1.080	3.734
8	.10	.50	8.639	24.399	1.080	3.050
16	.10	.50	17.278	48.798	1.080	3.050
24	.10	.50	25.917	73.197	1.080	3.050
32	.10	.50	34.556	97.595	1.080	3.050
8	.10	.70	8.640	24.619	1.080	3.077
16	.10	.70	17.280	49.237	1.080	3.077
24	.10	.70	25.920	73.856	1.080	3.077
32	.10	.70	34.559	98.475	1.080	3.077
8	.10	.90	8.641	34.460	1.080	4.308
16	.10	.90	17.282	68.920	1.080	4.308
24	.10	.90	25.922	103.381	1.080	4.308
32	.10	.90	34.563	137.841	1.080	4.308
8	.30	.45	10.237	36.428	1.280	4.553
16	.30	.45	20.475	72.856	1.280	4.553
24	.30	.45	30.712	109.283	1.280	4.553
32	.30	.45	40.950	145.711	1.280	4.553
8	.30	.60	10.235	28.924	1.279	3.615
16	.30	.60	20.470	57.847	1.279	3.615
24	.30	.60	30.705	86.771	1.279	3.615
32	.30	.60	40.940	115.695	1.279	3.615
8	.30	.75	10.242	28.186	1.280	3.523
16	.30	.75	20.484	56.372	1.280	3.523
24	.30	.75	30.727	84.558	1.280	3.523
32	.30	.75	40.969	112.744	1.280	3.523
8	.30	.90	10.251	35.733	1.281	4.467
16	.30	.90	20.503	71.466	1.281	4.467
24	.30	.90	30.754	107.199	1.281	4.467
32	.30	.90	41.005	142.931	1.281	4.467

TABLE II

NATURAL FREQUENCIES FOR TWO-HINGE ELASTIC-SEGMENT BLADE

$$\left[m_1 = m_2 = 0.6 \times 10^{-3} \frac{\text{lb-sec}^2}{\text{in.}^2};\ (EI)_1 = (EI)_2 = 3.15 \times 10^6 \text{ lb-in.}^2\right]$$

Ω, radians/sec	a_1	a_2	ω_1, radians/sec	ω_2, radians/sec	ω_3, radians/sec	ω_4, radians/sec	$\frac{\omega_1}{\Omega}$	$\frac{\omega_2}{\Omega}$	$\frac{\omega_3}{\Omega}$	$\frac{\omega_4}{\Omega}$
8	0.04	0.20	8.247	28.361	67.655	726.714	1.031	3.545	8.457	90.839
16	.04	.20	16.492	48.499	104.210	759.000	1.031	3.031	6.513	47.437
24	.04	.20	24.738	67.157	147.281	809.993	1.031	2.798	6.137	33.750
32	.04	.20	32.982	86.174	192.015	876.464	1.031	2.693	6.000	27.389
8	.04	.40	8.246	23.675	89.291	177.104	1.031	2.959	11.161	22.138
16	.04	.40	16.492	45.470	107.683	211.480	1.031	2.842	6.730	13.217
24	.04	.40	24.737	65.787	133.164	259.113	1.031	2.741	5.549	10.796
32	.04	.40	33.001	85.111	163.384	313.685	1.031	2.660	5.106	9.803
8	.04	.60	8.245	22.618	76.303	201.607	1.031	2.827	9.538	25.201
16	.04	.60	16.492	43.867	100.865	219.776	1.031	2.742	6.304	13.736
24	.04	.60	24.737	64.367	130.049	248.417	1.031	2.682	5.419	10.351
32	.04	.60	32.983	84.598	159.958	285.197	1.031	2.644	4.999	8.912
8	.04	.80	8.246	24.968	520.219	714.500	1.031	3.121	65.027	89.313
16	.04	.80	16.494	45.577	801.762	721.896	1.031	2.849	50.110	45.118
24	.04	.80	24.737	65.263	1,132.826	734.083	1.031	2.719	47.201	30.587
32	.04	.80	32.983	85.124	1,476.111	750.866	1.031	2.660	46.128	23.465
8	.10	.30	8.639	28.200	78.178	485.783	1.080	3.525	9.772	60.723
16	.10	.30	17.277	50.773	107.941	518.342	1.080	3.173	6.746	32.396
24	.10	.30	25.915	70.845	145.945	568.578	1.080	2.952	6.081	23.691
32	.10	.30	34.553	90.731	186.713	632.357	1.080	2.835	5.835	19.761
8	.10	.50	8.639	24.092	108.780	166.941	1.080	3.011	13.597	20.868
16	.10	.50	17.277	46.906	125.110	199.154	1.080	2.932	7.819	12.447
24	.10	.50	25.915	68.528	147.987	244.210	1.080	2.855	6.166	10.176
32	.10	.50	34.553	89.503	175.003	296.321	1.080	2.797	5.469	9.260
8	.10	.70	8.639	24.010	71.007	337.881	1.080	3.001	8.876	42.235
16	.10	.70	17.278	46.137	97.008	350.328	1.080	2.884	6.063	21.895
24	.10	.70	25.915	67.392	128.930	370.470	1.080	2.808	5.372	15.436
32	.10	.70	34.553	88.477	162.450	397.487	1.080	2.765	5.077	12.421
8	.10	.90	8.638	30.696	51.441	2,730.348	1.080	3.837	6.430	341.293
16	.10	.90	17.279	51.013	86.108	2,733.814	1.080	3.188	5.382	170.863
24	.10	.90	25.917	70.527	125.512	2,739.581	1.080	2.939	5.230	114.150
32	.10	.90	34.557	90.727	165.778	2,747.636	1.080	2.835	5.181	85.864
8	.30	.45	10.239	35.133	118.767	849.358	1.280	4.392	14.846	106.170
16	.30	.45	20.469	64.569	147.778	878.903	1.279	4.036	9.236	54.931
24	.30	.45	30.696	89.258	189.029	926.099	1.279	3.719	7.876	38.588
32	.30	.45	40.924	112.396	235.969	988.473	1.279	3.512	7.374	30.890
8	.30	.60	10.234	28.722	173.905	271.864	1.279	3.590	21.738	33.983
16	.30	.60	20.466	56.438	188.242	302.162	1.279	3.527	11.765	18.885
24	.30	.60	30.695	82.833	209.944	347.213	1.279	3.451	8.748	14.467
32	.30	.60	40.922	108.147	237.138	402.202	1.279	3.380	7.411	12.569
8	.30	.75	10.238	27.886	114.902	489.326	1.277	3.486	14.363	61.166
16	.30	.75	20.471	54.527	139.417	500.446	1.279	3.408	8.714	31.278
24	.30	.75	30.700	80.095	172.609	518.693	1.279	3.337	7.192	21.612
32	.30	.75	40.925	105.160	209.748	543.646	1.279	3.286	6.555	16.989
8	.30	.90	10.268	34.294	76.654	2,769.464	1.284	4.287	9.582	346.183
16	.30	.90	20.483	62.235	105.328	2,773.048	1.280	3.890	6.583	173.315
24	.30	.90	30.708	86.258	143.921	2,779.010	1.279	3.594	5.997	115.793
32	.30	.90	40.929	109.865	185.829	2,787.339	1.279	3.433	5.807	87.104

TABLE III

MODAL COEFFICIENTS FOR TWO-HINGE ELASTIC-SEGMENT BLADE

a_1	a_2	Ω	ω_n	n	$\frac{\varphi_1}{\varphi_2}$	$\frac{b_1}{R\varphi_2}$	$\frac{b_2}{R\varphi_2}$
0.04	0.40	8	8.246	1	40.588	-0.005	-0.011
.04	.40	8	23.675	2	-.451	-.003	-.016
.04	.40	8	89.291	3	-12.807	-2.327	14.819
.04	.40	8	177.04	4	-.752	.402	.272
.04	.40	16	16.492	1	48.194	-.018	-.031
.04	.40	16	45.470	2	-.422	-.007	-.048
.04	.40	16	107.683	3	-3.277	-.644	3.396
.04	.40	16	211.480	4	-.747	.381	.269
.04	.40	24	24.737	1	46.114	-.010	-.047
.04	.40	24	65.787	2	-.398	-.027	-.076
.04	.40	24	133.164	3	-2.145	-.455	2.041
.04	.40	24	259.113	4	-.743	.365	.267
.04	.40	32	33.001	1	41.747	-.031	-.052
.04	.40	32	85.111	2	-.381	-.012	-.096
.04	.40	32	163.384	3	-1.786	-.400	-1.611
.04	.40	32	313.685	4	-.741	.355	.266
.1	.50	32	34.553	1	-32.606	.076	-.085
.1	.50	32	89.503	2	-.324	-.017	-.060
.1	.50	32	175.003	3	.380	.383	-.983
.1	.50	32	296.321	4	-.746	.332	.352
.3	.60	32	40.922	1	7.615	-.027	-.023
.3	.60	32	108.147	2	-.357	-.009	-.038
.3	.60	32	237.138	3	.700	.357	-1.063
.3	.60	32	402.202	4	-.754	.269	.261

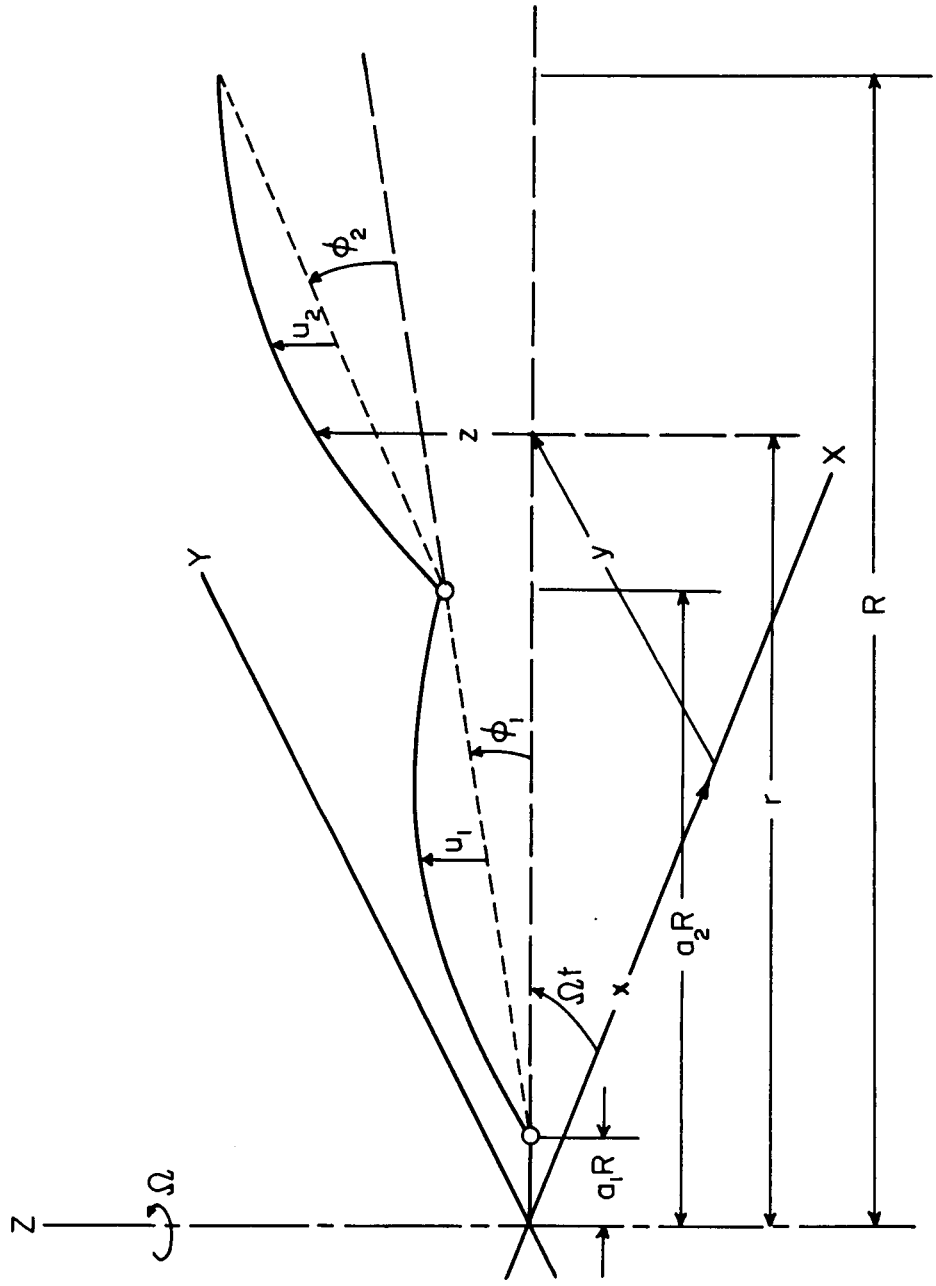

Figure 1.- Mathematical model of two-hinge elastic-segment blade.

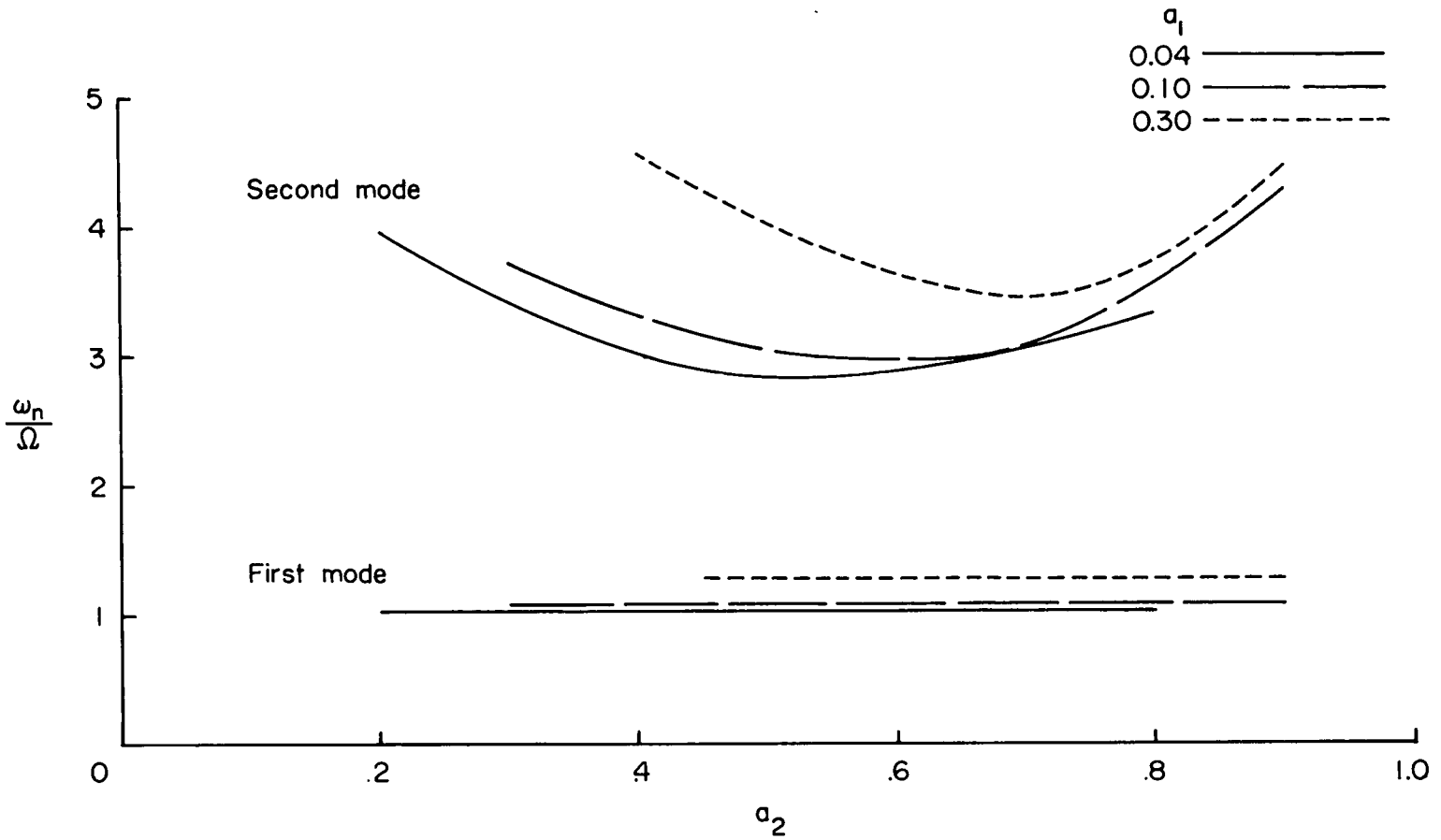

Figure 2.- Variation of frequency ratio with hinge locations for two-hinge, rigid-segment blade.

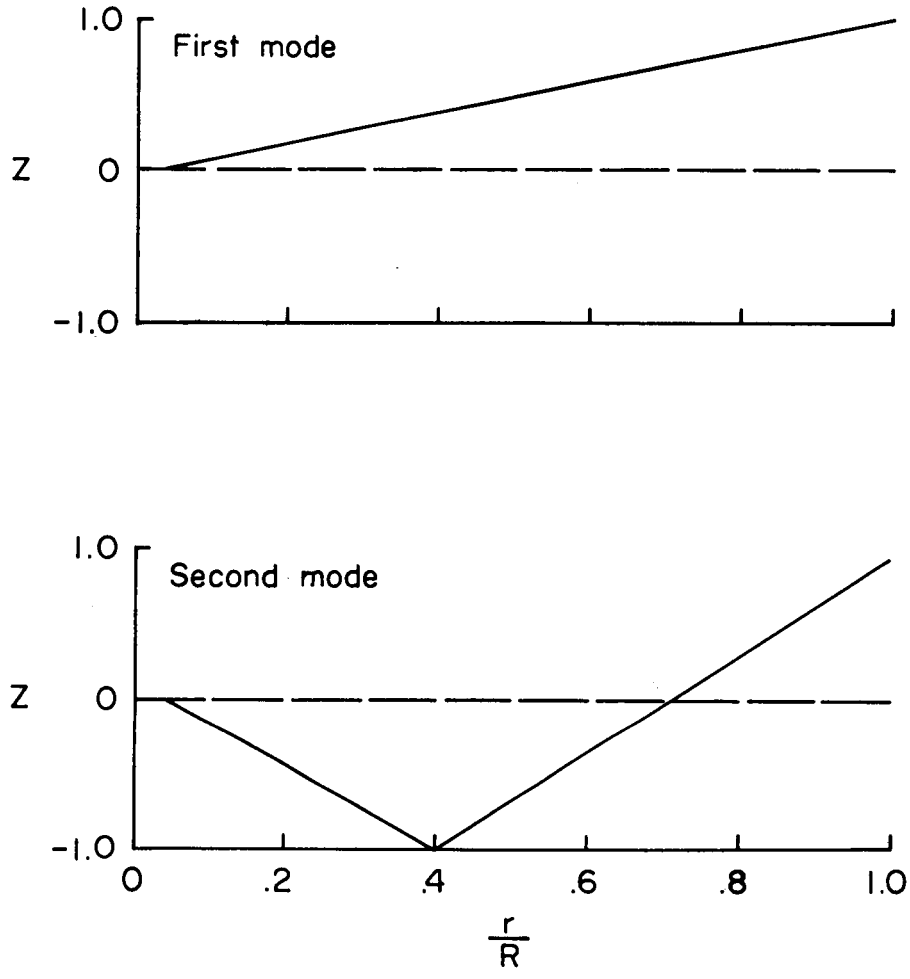

Figure 3.- Representative mode shapes for two-hinge, rigid-segment blade. $a_1 = 0.04$; $a_2 = 0.40$.

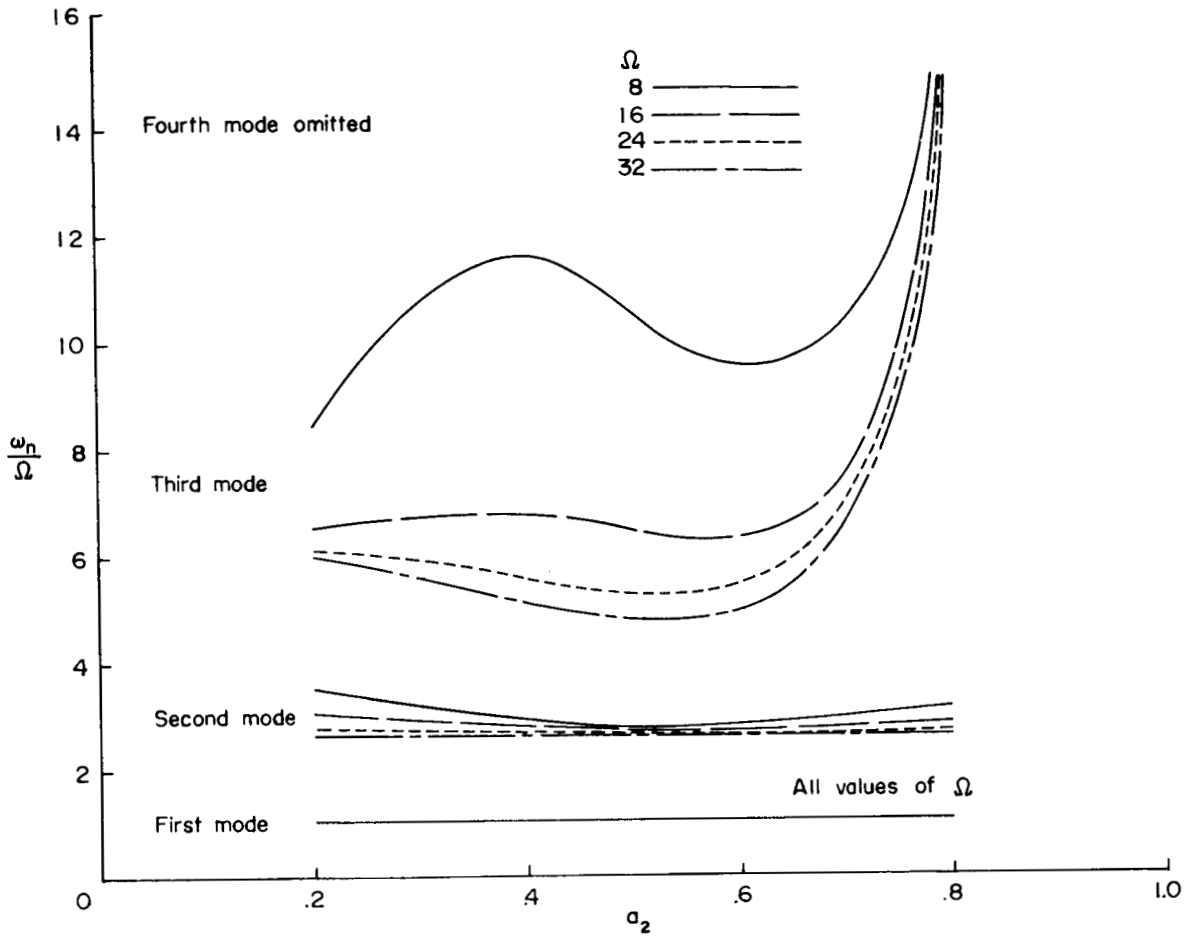

(a) $a_1 = 0.04$.

Figure 4.- Variation of frequency ratios with hinge locations and rotor speed for two-hinge elastic-segment blade.

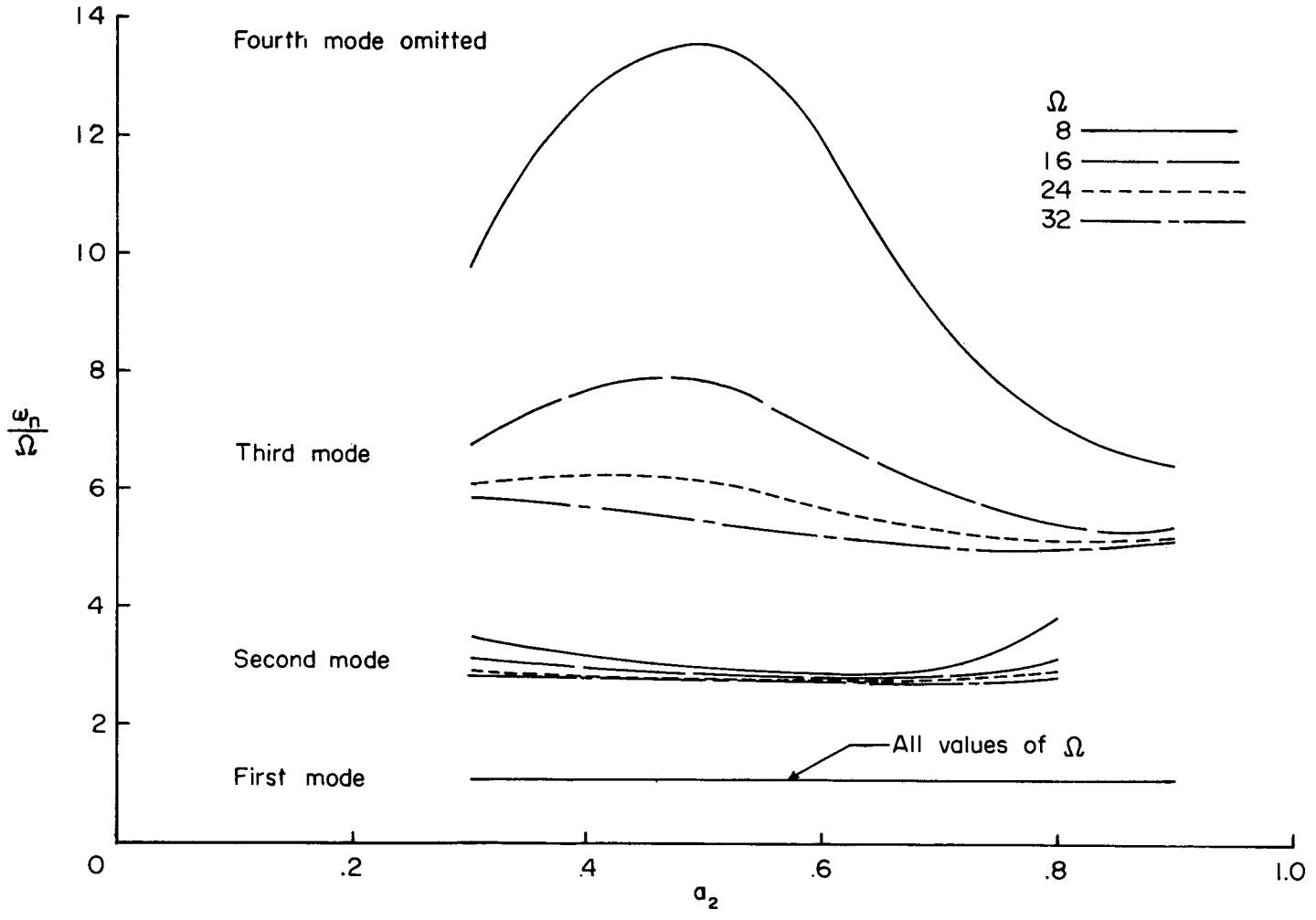

(b) $a_1 = 0.10$.

Figure 4.- Continued.

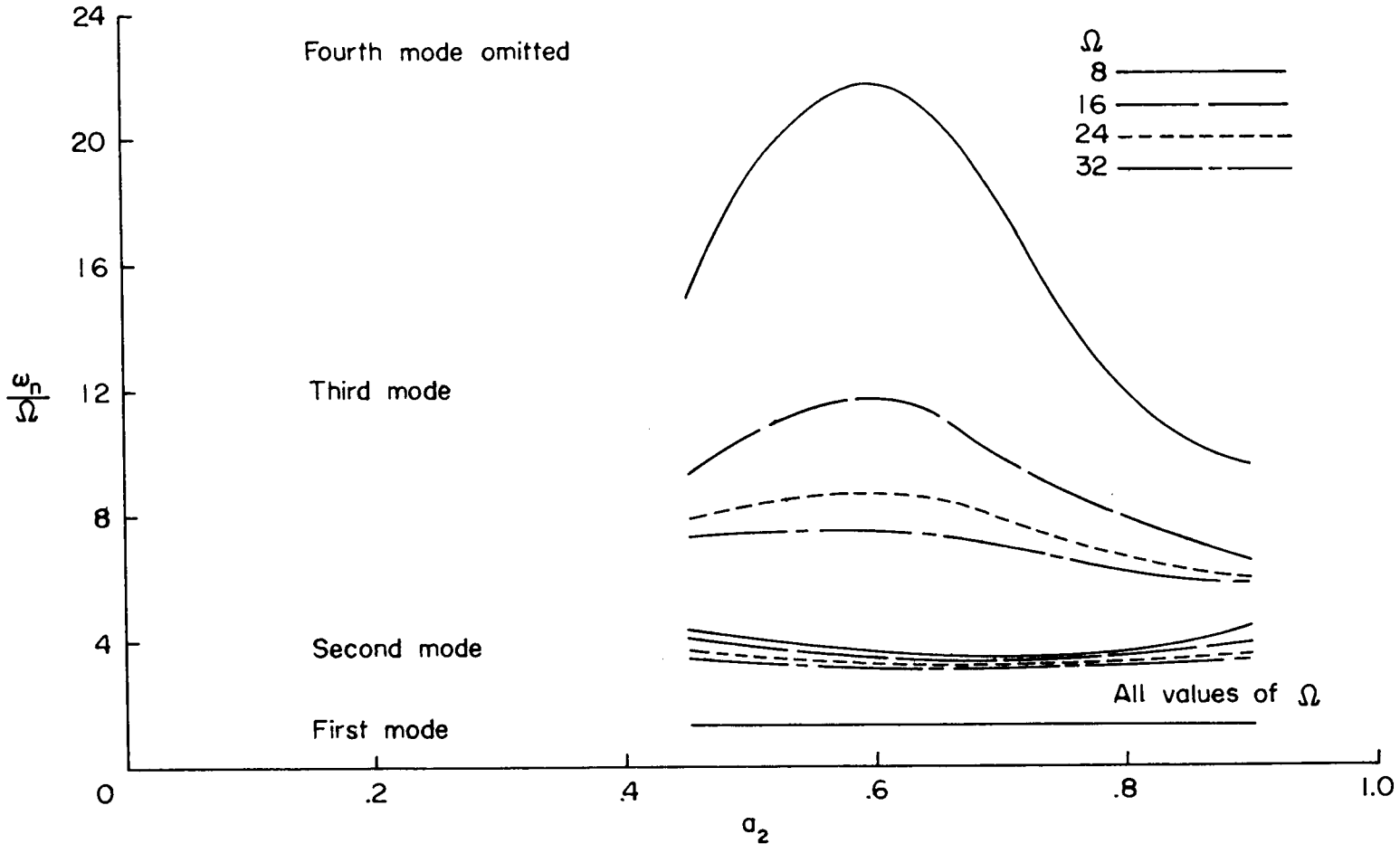

(c) $a_1 = 0.30$.

Figure 4.- Concluded.

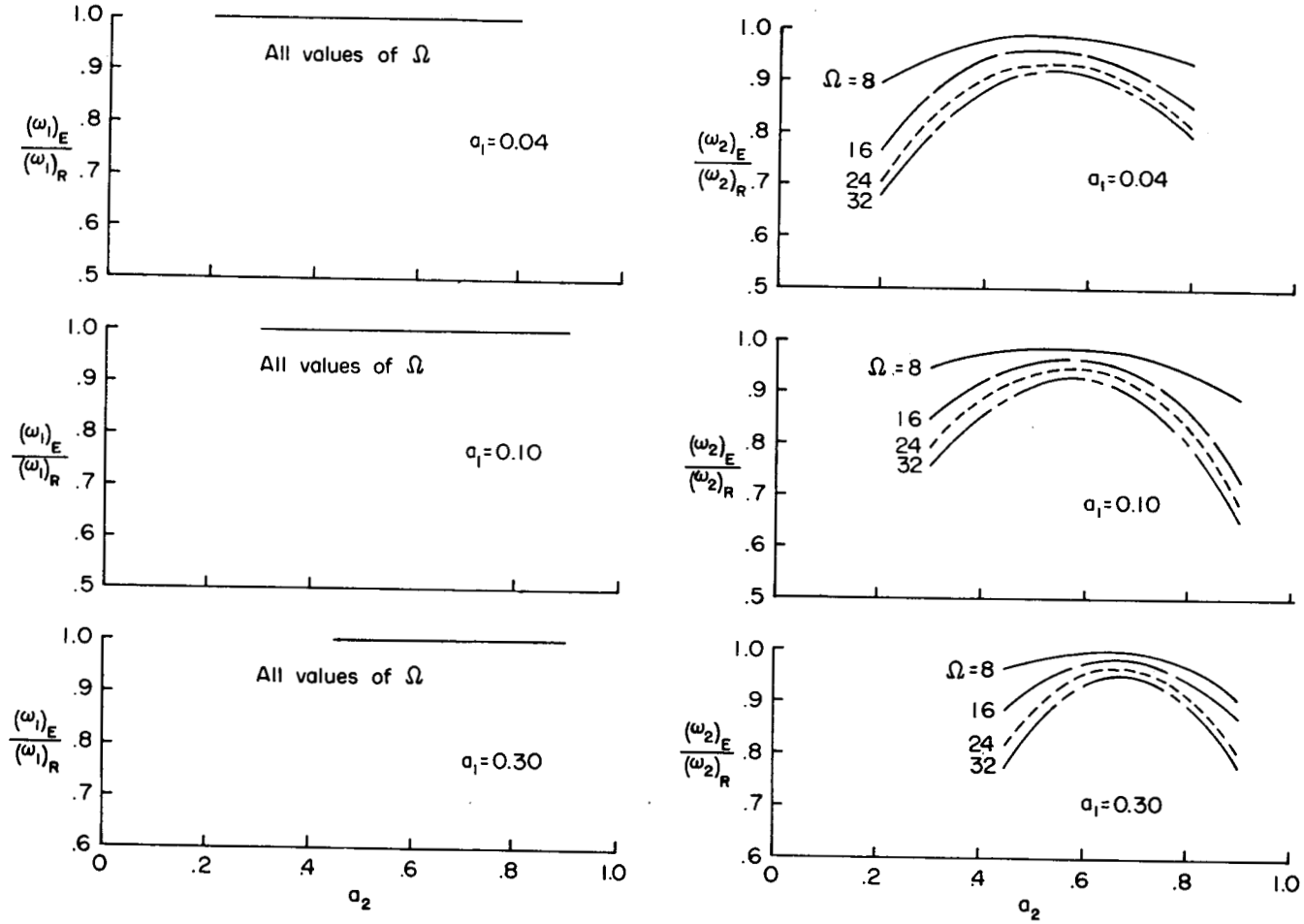

(a) First mode.

(b) Second mode.

Figure 5.- Effect of segment elasticity on the first two natural frequencies of a two-hinge rotor blade.

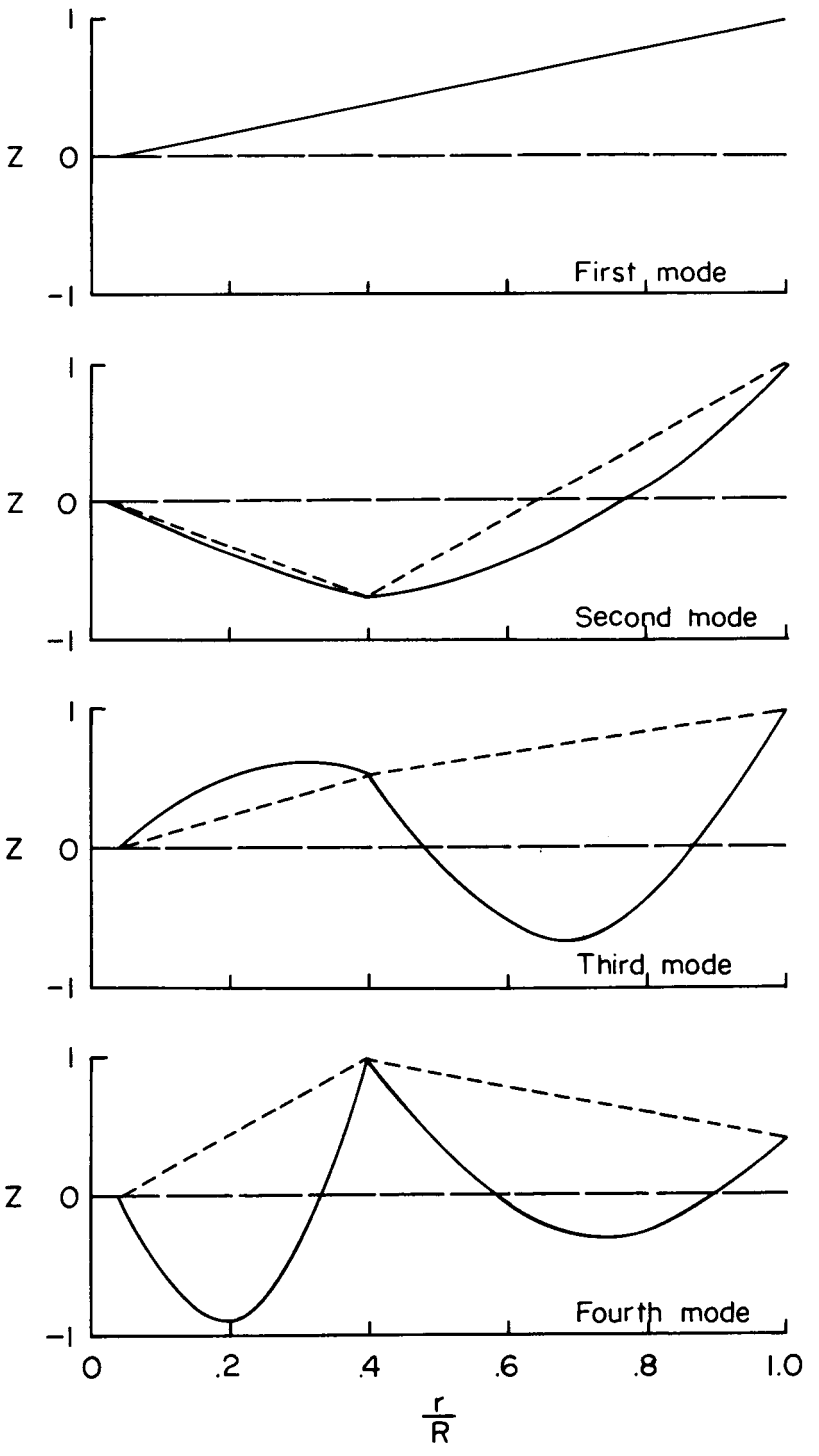

Figure 6.- Representative mode shapes for two-hinge elastic-segment blade. $a_1 = 0.04$; $a = 10$.

NASA TN D-633
National Aeronautics and Space Administration.
AN ANALYSIS OF THE FLAPWISE BENDING FREQUENCIES AND MODE SHAPES OF ROTOR BLADES HAVING TWO FLAPPING HINGES TO REDUCE VIBRATION LEVELS. George W. Brooks and H. Wayne Leonard. December 1960. 28p. OTS price, $0.75. (NASA TECHNICAL NOTE D-633)

The equations of motion are derived for a blade of variable mass and stiffness distribution. Solutions to the equations (natural frequencies and mode shapes) are presented for a typical blade of constant cross section having a wide range of hinge locations. The results show that the natural frequencies of the blades can be changed appreciably by varying the locations of the blade hinges, and that the ratios of natural frequency to rotor speed below a value of 6.0 are essentially constant for variations in rotor speed consistent with helicopter and VTOL applications.

Copies obtainable from NASA, Washington

I. Brooks, George W.
II. Leonard, H. Wayne
III. NASA TN D-633

(Initial NASA distribution: 3, Aircraft; 51, Stresses and loads.)

NASA

NASA TN D-633
National Aeronautics and Space Administration.
AN ANALYSIS OF THE FLAPWISE BENDING FREQUENCIES AND MODE SHAPES OF ROTOR BLADES HAVING TWO FLAPPING HINGES TO REDUCE VIBRATION LEVELS. George W. Brooks and H. Wayne Leonard. December 1960. 28p. OTS price, $0.75. (NASA TECHNICAL NOTE D-633)

The equations of motion are derived for a blade of variable mass and stiffness distribution. Solutions to the equations (natural frequencies and mode shapes) are presented for a typical blade of constant cross section having a wide range of hinge locations. The results show that the natural frequencies of the blades can be changed appreciably by varying the locations of the blade hinges, and that the ratios of natural frequency to rotor speed below a value of 6.0 are essentially constant for variations in rotor speed consistent with helicopter and VTOL applications.

Copies obtainable from NASA, Washington

I. Brooks, George W.
II. Leonard, H. Wayne
III. NASA TN D-633

(Initial NASA distribution: 3, Aircraft; 51, Stresses and loads.)

NASA

NASA TN D-633
National Aeronautics and Space Administration.
AN ANALYSIS OF THE FLAPWISE BENDING FREQUENCIES AND MODE SHAPES OF ROTOR BLADES HAVING TWO FLAPPING HINGES TO REDUCE VIBRATION LEVELS. George W. Brooks and H. Wayne Leonard. December 1960. 28p. OTS price, $0.75. (NASA TECHNICAL NOTE D-633)

The equations of motion are derived for a blade of variable mass and stiffness distribution. Solutions to the equations (natural frequencies and mode shapes) are presented for a typical blade of constant cross section having a wide range of hinge locations. The results show that the natural frequencies of the blades can be changed appreciably by varying the locations of the blade hinges, and that the ratios of natural frequency to rotor speed below a value of 6.0 are essentially constant for variations in rotor speed consistent with helicopter and VTOL applications.

Copies obtainable from NASA, Washington

I. Brooks, George W.
II. Leonard, H. Wayne
III. NASA TN D-633

(Initial NASA distribution: 3, Aircraft; 51, Stresses and loads.)

NASA

NASA TN D-633
National Aeronautics and Space Administration.
AN ANALYSIS OF THE FLAPWISE BENDING FREQUENCIES AND MODE SHAPES OF ROTOR BLADES HAVING TWO FLAPPING HINGES TO REDUCE VIBRATION LEVELS. George W. Brooks and H. Wayne Leonard. December 1960. 28p. OTS price, $0.75. (NASA TECHNICAL NOTE D-633)

The equations of motion are derived for a blade of variable mass and stiffness distribution. Solutions to the equations (natural frequencies and mode shapes) are presented for a typical blade of constant cross section having a wide range of hinge locations. The results show that the natural frequencies of the blades can be changed appreciably by varying the locations of the blade hinges, and that the ratios of natural frequency to rotor speed below a value of 6.0 are essentially constant for variations in rotor speed consistent with helicopter and VTOL applications.

Copies obtainable from NASA, Washington

I. Brooks, George W.
II. Leonard, H. Wayne
III. NASA TN D-633

(Initial NASA distribution: 3, Aircraft; 51, Stresses and loads.)

NASA